Molecular Dynamics Studies on the Prediction of Interface Strength of Cu (Metal)-$Cu_{50}Zr_{50}$ (Metallic glass) Metal Matrix Composites

A THESIS IN PARTIAL FULFILMENTS OF REQUIREMENTS FOR THE AWARD OF THE DEGREE OF

Master of Technology (Dual Degree)

Submitted to

NATIONAL INSTITUTE OF TECHNOLOGY, ROURKELA

by

Rakesh Nalla

710MM1126

Under the Guidance of

Dr. Natraj Yedla

DEPARTMENT OF METALLURGICAL & MATERIALS ENGINEERING

NATIONAL INSTITUTE OF TECHNOLOGY

ROURKELA-769008

INDIA

2015

CERTIFICATE

This is to certify that the thesis entitled Molecular Dynamics Studies on the Prediction of Interface Strength of Cu (Metal)-$Cu_{50}Zr_{50}$ (Metallic glass) Metal Matrix Composites by Rakesh Nalla in partial fulfilment of the requirements for the award of **Master of Technology** (Dual Degree) in Metallurgical and Material Science Engineering at National Institute of Technology, Rourkela, is an authentic work carried out by them under my supervision and guidance. To the best of my knowledge, the matter embodied in the thesis has not been submitted to any other university/institute for the award of any Degree or Diploma.

Dr. Natraj Yedla

Dept. of metallurgical Engineering

National Institute of Technology

ACKNOWLEDGEMENT

I take this opportunity to express my deep gratitude to Dr. Natraj Yedla, my guide, who provided me the initial motivation to work in this field. He kept on encouraging and inspiring me all through, sacrificing his valuable time & energy.

Also I express my sincere thanks to Mr. Pradeep Gupta (Phd scholar) who guided me throughout in running the simulations and also in producing the results.

I also express my sincere thanks to the Department of Metallurgical and Materials Engineering for all the help and coordination extended by the department.

I am also greatly thankful to all the staff members of the department and all my well-wishers.

Date:22-05-2015

Place:Rourkela

Rakesh Nalla

Roll No: 710MM1126

Dept. of Metallurgical and Materials Engineering

National Institute of Technology, Rourkela

ABSTRACT

The aim of this investigation is to predict the interface strength of metal (Cu-matrix)–metallic glass ($Cu_{50}Zr_{50}$-reinforcement) composites via molecular dynamics (MD) simulations. Simulation box size of 100 Å (x) × 110 Å (y) × 50 Å (z) is used for the investigation. At first Cu–$Cu_{50}Zr_{50}$ crystalline model is constructed with the bottom layer (Cu) of 50 Å and the top layer of 60 Å ($Cu_{50}Zr_{50}$) in height along y–direction. Thereafter, $Cu_{50}Zr_{50}$ metallic glass is obtained by rapid cooling at a cooling rate of 4×10^{12} s^{-1}. The interface model is then equilibrated at 300 K for 500 ps to relieve the stresses. EAM (Embedded Atom Method) potential is used for modelling the interaction between Cu–Cu and Cu–Zr atoms. The fracture strength of Cu–$Cu_{50}Zr_{50}$ model interface is determined by tensile (mode–I) and shear (mode–II) loading. Periodic boundary conditions are applied along z–direction for shear while along x– and z–directions for tensile tests. A timestep of 0.002 ps is used for all the simulations. Tensile and shear tests are carried out at varying strain rates (10^8 s^{-1}, 10^9 s^{-1} and 10^{10} s^{-1}) and temperatures (100K, 300 K and 500 K). The interface model is allowed for full separation under both the deformation modes. It is found that tensile as well as shear strength decrease with increase in temperature and increase with strain rate, as expected. Further, the maximum stress in shear is smaller than that in tensile at all strain rates and temperatures. Critical observations of the obtained results on Cu–$Cu_{50}Zr_{50}$ composites indicate better shear strengths as compared to the results of metal (matrix)-ceramic (reinforcement) composites available in the literature. Hence it can be concluded that metallic glass acts as a better reinforcement material than the popular ceramic reinforcements.

Key words: Molecular dynamics, tensile, shear, strain rate, temperature, interface.

Contents

Certificate ii
Acknowledgement iii
Abstract iv
List of figures 1
List of tables 2

CHAPTER ONE 3
1.1 Inroduction 3
1.1.1 Composite 3
1.1.2 Types of composites 3
1.1.2.1 Metal Matrix composites(MMCs) 3
1.1.2.2 Polymer Matrix composites(PMCs) 4
1.1.2.3 Ceramic Matrix composites(CMCs) 4
1.1.3 Applications of composites 4
1.1.4 Interface 4
1.1.5 Methods for studying the strength of the interface 5

1.1.5.1 Indentation hardness test ... 5
1.1.5.2 3-Point Bending Test ... 5
CHAPTER TWO ... 6
2.1 Literature Survey ... 6
2.2 Gaps in the literature ... 8
2.3 Objectives of the work ... 9
CHAPTER THREE ... 10
3.1 Modeling procedure ... 10
3.2 LAMMPS ... 11
3.3 Input script file for creating sample ... 12
3.4 Input script file for mode 1 (Tensile) deformation without crack ... 14
3.5 Input script file for mode 2 (Shear) deformation without crack ... 16
3.6 Input script file for mode 1 (Tensile) deformation with crack ... 18
3.7 Input script file for mode 2 (Shear) deformation with crack ... 20
3.8 Work Plan ... 22
CHAPTER FOUR ... 23
4.1 Results and Discussions ... 23
4.2 Deformation (Tensile and Shear) studies of the Cu –CuZr interface ... 23
4.3 Effect of strain rate on the interface strength ... 24
4.3.1 Atomic positions snap shots (Mode I without crack) ... 26
4.3.2 Atomic positions snap shots (Mode I with crack) ... 28
4.3.3 Atomic positions snap shots (Mode II without crack) ... 30
4.3.4 Atomic positions snap shots (Mode II with crack) ... 32
4.4 Effect of temperature on interface strength ... 33
CONCLUSIONS ... 37
REFERENCES ... 38

List of Figures

Fig No.	Caption	Page
1	Atomic snapshot of interface (a) without crack, (b) with crack	24
2	Stress-Strain plot for Mode-I without crack, Cu50Zr50 metallic glass reinforced in Cu Metal matrix.	25
3a	Atomic snapshot at different strains of the model without crack under Mode-I deformation	26
3b	Atomic snapshot at different strains of the model without crack under Mode – I deformation.	26
4	Stress-Strain plot for Mode-I with crack, Cu50Zr50 metallic glass reinforced in Cu Metal matrix.	27
5a	Atomic snapshot at different strains of the model with crack under Mode-I deformation.	28
5b	Atomic snapshot at different strains of the model with crack under Mode-I deformation.	29
6	Stress-Strain plot for Mode-II without crack, Cu50Zr50 metallic glass reinforced in Cu Metal	30
7a	Atomic snapshot at different strains of the model without crack under Mode –II deformation.	31
7b	Atomic snapshot at different strains of the model without crack under Mode – II deformation.	31
8	Stress-Strain plot for Mode-II with crack, Cu50Zr50 metallic glass reinforced in Cu Metal matrix.	32
9a	Atomic snapshot at different strains of the model with crack under Mode-II deformation.	33
	Atomic snapshot at different strains of the model with crack under Mode-II deformation.	33
10	Stress-Strain plot for Mode-I without crack, Cu50Zr50 metallic glass reinforced in Cu Metal	34
11	Stress-Strain plot for Mode-I with crack, Cu50Zr50 metallic glass reinforced in Cu Metal	35
12	Stress-Strain plot for Mode-II without crack, Cu50Zr50 metallic glass reinforced in Cu Metal	36
13	Stress-Strain plot for Mode-II with crack, Cu50Zr50 metallic glass reinforced in Cu Metal	37

List of Tables

1 Details of studies 22

CHAPTER 1

1.1 INTRODUCTION

1.1.1 COMPOSITE

Composite is a blend of two materials, where one of the materials is called the reinforcing phase, made up of particles or fibers that are embedded in the matrix phase. The second phase is called matrix phase. The function of the matrix phase is to transfer stress between the reinforcement phases [1]. Composite is a heterogeneous mixture of two or more materials where the individual properties of the materials are preserved unlike an alloy. Composite is a combination of two or more phases, one phase is stronger and is called reinforcement and the other is a weaker phase called the matrix. The reinforcing phase is normally used to increase the stiffness and strength of the matrix phase.

1.1.2 TYPES OF COMPOSITES

1.1.2.1 METAL MATRIX COMPOSITES (MMCs)

The composite material where at least one constituent is metal and the other material may be either metal or any other material. These metal matrix composites are made by dispersion of reinforcing material in the metal matrix. In structural applications, lighter metals are used as matrix providing support to the reinforcements [2]. Cobalt and nickel alloy matrix is used for high temperature applications.

1.1.2.2 POLYMER MATRIX COMPOSITES (PMCs)

These composites consist of polymer matrix with glass, aramid and boron fibers as reinforcing materials. Polymer matrix materials in comparison to MMC's and CMC's are manufactured with ease. The secret of their wide application lies in the ease of their production and their light weight. Glass fiber reinforced polymers is most widely used composite materials. One of the main drawbacks of the PMCs' is low service temperature[3].

1.1.2.3 CERAMIC MATRIX COMPOSITES (CMCs)

These polymers have ceramic materials as the matrix with any other reinforcing materials. Ceramic materials have high strength, good high-temperature properties and low density. The use of ceramic materials is limited because of certain drawbacks[4]. They cannot withstand tensile loading because of poor ductility and low plasticity. Ceramics materials are brittle. This is because of the inability to dissipate energy. So in order to increase the toughness of these materials, ceramic matrix composites are used.

1.1.3 APPLICATIONS OF COMPOSITES

Composites are used in the manufacture of variety of products like sports goods, rockets, missiles, spacecraft, satellites and various automobile components. Carbon fiber reinforced plastic is used in cases of limb deformity. Chemical industry uses the composites for valves, containers, pressure vessels etc. Lightweight, high-strength carbon, kevlar and glass-fiber composites are used in military aircrafts [5]. Extensively composites are used in sports goods industry in the form of cricket bats, surfing boards, bicycles, tennis rackets etc. The use of composite materials has significantly increased in the recent times.

1.1.4 INTERFACE

The surface between the matrix phase and the reinforcing phase is called interface. Interface is a boundary through which the different properties of the materials such as elastic modulus, density, and concentration change, etc change. The properties of the composite materials depends on the i) matrix phase, ii) reinforcing phase and iii) interface between the matrix and the interface. The interface plays a vital role in determining the mechanical properties of the composite. This is because of the large surface area occupied by the interface. Therefore the interface between the matrix and the reinforcement plays a crucial role in determining the resultant properties of the composite and the strength of the composite depends on the strength of the interface.

1.1.5 METHODS FOR STUDYING THE STRENGTH OF THE INTERFACE

1.1.5.1 INDENTATION HARDNESS TEST

Indentation hardness tests are utilized as a part of mechanical building to focus the hardness of a material to distortion. A few such tests exist, wherein the analysed material is indented until an impression is framed; these tests can be performed on a naturally visible or tiny scale. At the point when testing metals, space hardness corresponds sprightly with tractable strength. This connection allows financially imperative non-destructive testing of mass metal conveyances with lightweight, even compact hardware, for example, hand-held Rockwell hardness analysers.

1.1.5.2 3-POINT BENDING TEST

The 3-point bending test enables the calculation of young's modulus in bending, flexural stress, stress-strain behaviour of the material. The fundamental favourable position of a three point flexural test is the simplicity of the sample preparation and testing. Then again, this system has additionally a few drawbacks: the after effects of the testing strategy are touchy to sample and stacking geometry and strain rate.

CHAPTER 2

2.1 LITERATURE SURVEY

Composite consists of a strong phase (reinforcement) and a weak phase (matrix). So the strength of the composite depends on the degree of compatibility between the two regions. Depending on the extent of bonding and the interface thickness between these two phases, the deformation behavior varies. In this work, the interface is modeled using finite element method to analyse the behavior of metal matrix composites under deformation. A thin layer of interface is modeled using an artificial material. Different samples of the material with different stiffness and different volume fractions are used to vary the interaction at the interface. It is found that the composite provides greater strength than the traditional materials. This is significantly realized for higher volume fraction of reinforcement and large area of the interface. The flow curves match with the experimental curves [6]**.** The enhancing use of metal matrix composites in different areas of interest makes it necessary for the prediction of mechanical properties from the known parameters. In this work investigation of the effect of interface strengths on the mechanical behavior of composite at different loading conditions is done. Failure mechanisms during the loading process: ductile failure in metal matrix, brittle failure in SiC particles and interface debonding between matrix and particles. The damage models are developed to simulate the failure in the composite. The simulation results show that particle arrangements plays little role in the stress–strain relationships before damage initiates. However, the particle arrangements in the micromechanical models do play a significant role in the maximum strengths and corresponding failure strain of MMC. Under uniaxial tensile loading, the strength of weak interface is higher than that of strong interface, while the failure strains with weak interface are lower than that with strong interface [7]. In the recent years, the use of materials made up of metals and ceramics significantly increased because of their versatile properties which makes them suitable for application in various ways. Despite the increasing use of these materials, the mechanical properties of metal-ceramic interfaces is not properly understood. In this work, a cohesive law is established for metal-ceramic interfaces using Vander Waal's force. Equations for calculation of shear and tensile stresses are derived from the grain size, volume density and also from the parameters in Vander Waal's force. The cohesive law is governed by tensile cohesive stress, shear cohesive stress and cohesive energy. This helps in understanding the interface strength of metal ceramic composites. This law is very helpful for the interfaces which have Vander Waal's force as the predominant mechanism of interaction [8]. The interface between the matrix and reinforcement plays a crucial role in deciding the resultant properties of composite. Strong interface ensures efficient load transfer from reinforcement to matrix which affects properties such as stiffness, creep and fatigue. Here, a cohesive zone law is modelled by MD simulations in order to generate traction-separation law for ductile brittle interface in Mode I and Mode II deformations at elevated temperatures. It is found that the traction-separation law is consistent with the existing models [9]. With the advancement of modern technology, the need for new engineering materials for automobile industries became necessary leading to the development of MMC's. Aluminium particularly has very high strength to weight ratio. The interface is the critical region in determining the properties of composites. The problem with the interface is the improper wettability of the reinforcement with the matrix. Coating of the reinforcements is one of the technique to improve the interfacial bonding. This work coating on reinforcements such as carbon/graphite, showed improvement in the interactions at the interface. The metal coatings improved the wettability of the matrix and reinforcement. It is economical but leads to change in the composition of the matrix. Ceramic coatings reduce the wettability of the reinforcement with matrix and most of them are quite expensive [10]. Metallic glasses have a unique set of properties including high yield strength and large elastic limit and also good resistance to corrosion. Taking these properties into consideration, the metallic glasses can be used as reinforcements in metal matrix composites (MMCs), which are blend of high-strength glassy phase and a soft metallic matrix. The mechanical properties of Al-based composites reinforced with different volume fractions of $Fe_{49.9}Co_{35.1}Nb_{7.7}B_{4.5}Si_{2.8}$ glassy particles are investigated under tensile loading [11]. Metallic glasses are assessed to be good structural materials. Although they have restricted applications in comparision with conventional materials, their outstanding properties make them useful for wide range of applications like in micro electro-mechanical system devices. They are made to perform better at high temperatures, designed to have better mechanical and thermal fatigue and creep resistance. MMc's in comparision to PMC's have amazing resistance to flame, moisture and hence can withstand high temperatures [12]. The solubility of carbon in copper is less at high temperatures. Hence the wettability of carbon fibres with copper is low. This low wettability does not allow proper fabrication of composite. Thus taking this into consideration, studies of the interfaces by using the Metallic Glasses as reinforcement materials is done and it is found that there is improvement in bond strength at the interface.[13]

2.2 GAPS IN THE LITERATURE

A significant progress is made in the usage of composite materials in the recent times. However, in comparison to all other composites, the research on metal-metallic glass composites has drawn less attention. There are seldom experimental and simulation deformation studies reported on the metal-metallic glass composites. So, in view of this, the present study is broadly aimed to study the following:

a) Interface strength of the metal (Cu)-metallic glass ($Cu_{50}Zr_{50}$) composite interface by performing molecular dynamics (MD) simulations.
b) Crack behaviour along the Cu-CuZr interface subjected to different loading conditions and temperatures.

2.3 OBJECTIVES OF THE WORK

a) To create Cu (metal)-CuZr (metallic glass) model interface.

b) To carry out Mode I (tensile) and Mode II (shear) deformation studies of the Cu (metal)-CuZr(metallic glass) interface .

c) To investigate the crack propagation behaviour at the Cu (metal)-CuZr (metallic glass) interface.

d) To carryout mode-I (tensile) and mode-II (shear) deformation studies of Cu (metal)-CuZr (metallic glass) interface with crack.

e) To study the effect of temperature (100 K, 300 K, 500 K) and strain rates (10^8 s^{-1}, 10^9 s^{-1}, and 10^{10} s^{-1}) on the interface strength during mode-I and mode-II loading conditions.

CHAPTER 3

3.1 MODELING PROCEDURE [12]

Molecular dynamics is a simulation technique where the positions of a set of interacting atoms and molecules of a system is determined by using the equations of motion. The atoms and molecules of the system are allowed to interact for the period of time giving a view of their motion. The trajectories of the interacting particles are determined by solving Newton's equations of motion where forces between the particles and the potential energy are defined by molecular mechanics force fields. The Newton's equation of motion can be expressed as follows:

$$F=m_i a_i \qquad (1)$$

$$a_i = d^2 r_i / dt^2 \qquad (2)$$

where F is the force between the interacting particles, m_i = mass of each particle (considering the homogenous system, mass of each particle is same), a_i = acceleration of each particle and r_i = particle position.

Given an initial set of positions and velocities, the subsequent time evolution through which the particle interaction and movement takes place can be completely determined. During simulations atoms and molecules will 'move' in the computer, bumping into each other during interaction, vibrating about a mean position (if constrained), or wandering around (if the system is fluid), oscillating in waves in concert with their neighbours, perhaps evaporating away from the system if there is a free surface, and so on, in a way similar to what real atoms and molecule would do.

The initializations of MD simulations starts with initializing the positions and velocities of atoms and after that the total energy is being calculated which include bond energy, torsional energy, bond angle energy, non-bond energy. Then the forces on the atoms are calculated. Subsequently, atoms are moved and Newton's equation of motion is integrated to obtain the atomic trajectory.

Since any molecular system contains a large number of micro-particles, atoms or molecules. It is quite impractical and most of the times impossible to characterize the properties of such a vast system analytically. In this case MD simulation comes handy to solve this problem by using numerical methods. In order to get the simulation results to be error free, calculation are carried out by the machine (computer) selecting a proper algorithm implemented in a suitable programming language. In this way, complexity can be introduced and more realistic systems can be investigated, achieving a better understanding of real experiments. Due to its important commercial applications, this simulation technique is now gaining much more popularity.

3.2 LAMMPS

- LAMMPS is an acronym for Large scale Molecular Massively Parallel Simulator. This is the basic code required to do materials simulation.
- LAMMPS consists of potentials for soft materials and solid-state materials and many more kind of materials
- LAMMPS can be used to model atoms or as a parallel particle simulator.
- For computational efficiency LAMMPS uses neighbour lists to keep track of nearby particles.
- This code is written with the help of c++. The designing structure of the code is so flexible that it can be easily modified and extended with new applications.
- A set of pre and post-processing tools are also packaged with LAMMPS, some of which can convert input and output files to/from formats used by other codes.
- OVITO is a molecular visualizations/graphics program designed for the display and analysis of molecular assemblies.
- OVITO can display any number of structures using a wide variety of rendering styles and coloring method.

In this project work, all the simulations have been performed using LAMMPS and resulting models and structures have been analyzed and processed using OVITO Visualization program.

3.3 INPUT SCRIPT FILE FOR CREATING SAMPLE

```
# Cu-CuZr interface studies
units          metal
echo           both
atom_style     atomic
dimension      3
```

```
boundary        p p p
region          box block 0 100 0 110 0 50  units box
create_box      3 box

lattice          fcc 3.61
region           Cu block 0 100 0 50  0 50 units box
create_atoms     1 region Cu units box
group            solid region Cu


lattice          fcc 3.61
region           CuZr_glass block 0 100 60 110  0 50 units box
create_atoms     2 region CuZr_glass units box
set              region CuZr_glass type/fraction 3 0.5 12393


group          glass region CuZr_glass
group          entire union solid glass

timestep       0.002

pair_style          eam/fs
pair_coeff           * * Cuzr_mm.eam.fs Cu Cu Zr


thermo      1000
velocity     all create 300 8728007 rot yes mom yes dist gaussian


# Energy Minimization
minimize    1.0e-3 1.0e-4 10000 10000
```

```
thermo_style     custom step temp  vol press pe ke etotal

dump     1 all atom 40000 dump.Cu-CuZr_interface.lammpstrj
dump_modify 1 scale no
log logCu-CuZr_interface.data

fix             1 glass npt temp 300 2000 0.01 iso 0.0 0.0 0.1

run             10000
unfix           1

fix             1 glass npt temp 2000 2000 0.01 iso 0.0 0.0 0.1

run             50000
unfix           1

fix             1 glass npt temp 2000 270 0.01 iso 0.0 0.0 0.1
run             100000
unfix           1
```

3.4 INPUT SCRIPT FILE FOR MODE I (TENSILE) DEFORMATION WITHOUT CRACK

```
# 3d metal tensile simulation

units                  metal
boundary               s s p
echo                   both
atom_style             atomic

read_data              cuzr.dat

pair_style             eam/fs
pair_coeff             * * CuZr_mm.eam.fs Cu Cu Zr
```

```
#region

region   1  block  -3 103   -3 30   -2 52 units box
region   2  block  -3 103   60  114  -2 52 units box

group          lower region 1
group          upper region 2
group          boundary union lower upper
group          mobile subtract all boundary


compute      csym all centro/atom fcc
compute      peratom all pe/atom

# Energy Minimization

  minimize            1.0e-9 1.0e-9 1000 10000

# equilibrate

velocity              mobile create 100.0 5812775
fix                   1 all nvt temp 100 100 0.01
fix                   2 boundary setforce 0.0 0.0 0.0



 timestep             0.002

# shear

velocity              upper set  0.0 0.003 0.0
velocity              mobile ramp vy 0.0 0.003 y 30 60 sum no units box

# output

dump              1 all custom 100 dump1.tensile_check2*.lammpstrj id type x y z


# stress calculation

compute           10 mobile stress/atom


compute           20 mobile reduce sum c_10[2]


#large 150000 vol;
```

variable   stress equal c_20/(3*150000)

variable   stress_MPa equal v_stress/10

#log file

log logcu_cuzr5050_tensile_ramp_check2.dat

thermo   1000
thermo_style   custom step temp v_stress v_stress_MPa

run   500000

3.5 INPUT SCRIPT FILE FOR MODE II (SHEAR) DEFORMATION WITHOUT CRACK

3d metal shear simulation

units   metal
boundary   s s p
echo   both
atom_style   atomic

read_data   cuzr.dat

pair_style   eam/fs
pair_coeff   * * CuZr_mm.eam.fs Cu Cu Zr

#region

```
region   1  block  -3 103   -3 30   -2 52 units box
region   2  block  -3 103   60  114  -2 52 units box

group         lower region 1
group         upper region 2
group         boundary union lower upper
group         mobile subtract all boundary


#region              my cylinder z 50 50 10 0 54 units box
#delete_atoms     region my

compute      csym all centro/atom fcc
compute      peratom all pe/atom

# Energy Minimization

  minimize            1.0e-4 1.0e-4 1000 10000

# equilibrate

velocity              mobile create 300.0 5812775
fix                   1 all nvt temp 300 300 0.01
fix                   2 boundary setforce 0.0 0.0 0.0


 timestep              0.002



# shear

velocity              upper set  0.01 0.0 0.0
velocity              mobile ramp vx 0.0 0.01 y 30 60 sum no units box

# output

dump                  1 all custom 100 dump1.shear_10^8_check2*.lammpstrj id type x y z



# stress calculation

compute             10 mobile stress/atom

compute              20 mobile reduce sum c_10[4]
```

```
#large 150000 vol;

variable        stress equal c_20/(3*150000)

variable        stress_MPa equal v_stress/10

variable        strain equal (xhi-104)/104


#log file

log logcu_cuzr5050_shear_10^8_check2.dat

thermo        2500
thermo_style   custom step temp v_stress v_stress_MPa v_strain


run           500000
```

3.6 INPUT SCRIPT FILE FOR MODE I (TENSILE) DEFORMATION WITH CRACK

```
# 3d metal tensile simulation

units                  metal
boundary               s s p
echo                   both
atom_style             atomic

read_data              cuzr.dat

pair_style             eam/fs
pair_coeff             * * CuZr_mm.eam.fs Cu Cu Zr

#region

region   1  block  -3 103   -3 30   -2 52 units box
region   2  block  -3 103   60  114  -2 52 units box

group          lower region 1
```

```
group          upper region 2
group          boundary union lower upper
group          mobile subtract all boundary


region              my cylinder z 50 50 10 0 54 units box
delete_atoms     region my



compute      csym all centro/atom fcc
compute      peratom all pe/atom

# Energy Minimization

  minimize           1.0e-9 1.0e-9 1000 10000

# equilibrate

velocity             mobile create 100.0 5812775
fix                  1 all nvt temp 100 100 0.01
fix                  2 boundary setforce 0.0 0.0 0.0


 timestep             0.002

# tensile

velocity             upper set  0.0 0.003 0.0
velocity             mobile ramp vy 0.0 0.003 y 30 60 sum no units box

# output

dump                1 all custom 100 dump1.tensile_check2*.lammpstrj id type x y z



# stress calculation

compute              10 mobile stress/atom


compute              20 mobile reduce sum c_10[2]


#large 150000 vol;

variable        stress equal c_20/(3*150000)
```

```
variable        stress_MPa equal v_stress/10


#log file

log logcu_cuzr5050_tensile_ramp_check2.dat

thermo       1000
thermo_style   custom step temp v_stress v_stress_MPa


run            500000
```

3.7 INPUT SCRIPT FILE FOR MODE II (SHEAR) DEFORMATION WITH CRACK

```
# 3d metal shear simulation

units                   metal
boundary                s s p
echo                    both
atom_style              atomic

read_data               cuzr.dat

pair_style              eam/fs
pair_coeff              * * CuZr_mm.eam.fs Cu Cu Zr

#region

region   1  block  -3 103   -3 30   -2 52 units box
region   2  block  -3 103   60  114  -2 52 units box

group                lower region 1
group                upper region 2
group          boundary union lower upper
group          mobile subtract all boundary
```

```
region              my cylinder z 50 50 10 0 54 units box
delete_atoms     region my

compute      csym all centro/atom fcc
compute      peratom all pe/atom

# Energy Minimization

  minimize           1.0e-4 1.0e-4 1000 10000

# equilibrate

velocity              mobile create 300.0 5812775
fix                   1 all nvt temp 300 300 0.01
fix                   2 boundary setforce 0.0 0.0 0.0

#fix                  3 lower temp/rescale 10 300.0 300.0 10.0 1.0

 timestep             0.002

# shear

velocity              upper set  0.01 0.0 0.0
velocity              mobile ramp vx 0.0 0.01 y 30 60 sum no units box

# output

dump                 1 all custom 100 dump1.shear_10^8_check2*.lammpstrj id type x y z


# stress calculation

compute             10 mobile stress/atom

compute              20 mobile reduce sum c_10[4]


#large 150000 vol;

variable       stress equal c_20/(3*150000)

variable       stress_MPa equal v_stress/10

variable       strain equal(xhi-104)/104

#log file
```

```
log logcu_cuzr5050_shear_10^8_check2.dat

thermo        2500
thermo_style   custom step temp v_stress v_stress_MPa


run    500000
```

Deformation studies in both cases Mode I and Mode II (with crack & without crack) are carried out at different strain rates (10^8 s^{-1} , 10^9 s^{-1} , 10^{10} s^{-1}) and different temperatures (100K, 300K, 500K) using the above codes.

3.8 WORK PLAN

The following Table 1 gives the details of the simulation studies that will be carried out on Cu-Cu-Zr interface.

Table 1: Details of studies

Alloy model	**Mode of deformation**	**Strain rate**	**Temperature**
Cu-Cu-Zr	Mode-I	10^8 s^{-1} 10^9 s^{-1} 10^{10} s^{-1}	100 K , 300 K, 500 K 100 K , 300 K, 500 K 100 K , 300 K, 500 K
Cu-Cu-Zr	Mode-II	10^8 s^{-1} 10^9 s^{-1} 10^{10} s^{-1}	100 K , 300 K, 500 K 100 K , 300 K, 500 K 100 K , 300 K, 500 K
With center crack at the interface			
Cu-Cu-Zr	Mode-I	10^8 s^{-1} 10^9 s^{-1} 10^{10} s^{-1}	100 K , 300 K, 500 K 100 K , 300 K, 500 K 100 K , 300 K, 500 K
Cu-Cu-Zr	Mode-II	10^8 s^{-1} 10^9 s^{-1} 10^{10} s^{-1}	100 K , 300 K, 500 K 100 K , 300 K, 500 K 100 K , 300 K, 500 K

CHAPTER 4

4.1 RESULTS AND DISCUSSIONS

MD simulations of Mode-I and Mode-II studies on the Cu- $Cu_{50}Zr_{50}$ interface with crack and without crack have been studied. The tests were conducted at varying strain rates (1×10^{8} s^{-1}, 1×10^{9} s^{-1} and 1×10^{10} s^{-1}) and temperatures (100K, 300K and 500K) to investigate the deformation behaviour and response on the mechanical properties such as yield point, and maximum load the interface can withstand.

4.2 DEFORMATION (TENSILE AND SHEAR) STUDIES OF THE Cu (METAL)-CuZr (METALLIC GLASS) INTERFACE

The model was deformed along Y-axis (Tensile, Mode-I) and X-axis (Shear, Mode-II). The deformation was done at different strain rates i.e., 1×10^{8} s^{-1}, 1×10^{9} s^{-1} and 1×10^{10} s^{-1} and at different temperatures in the range of 100 K-500 K to understand the stress-strain behaviour and response to the mechanical properties. Fig 1 shows the atomic snapshot of the Interface without crack (Fig. 1a) and with crack (diameter 10 Å) (Fig.1b).

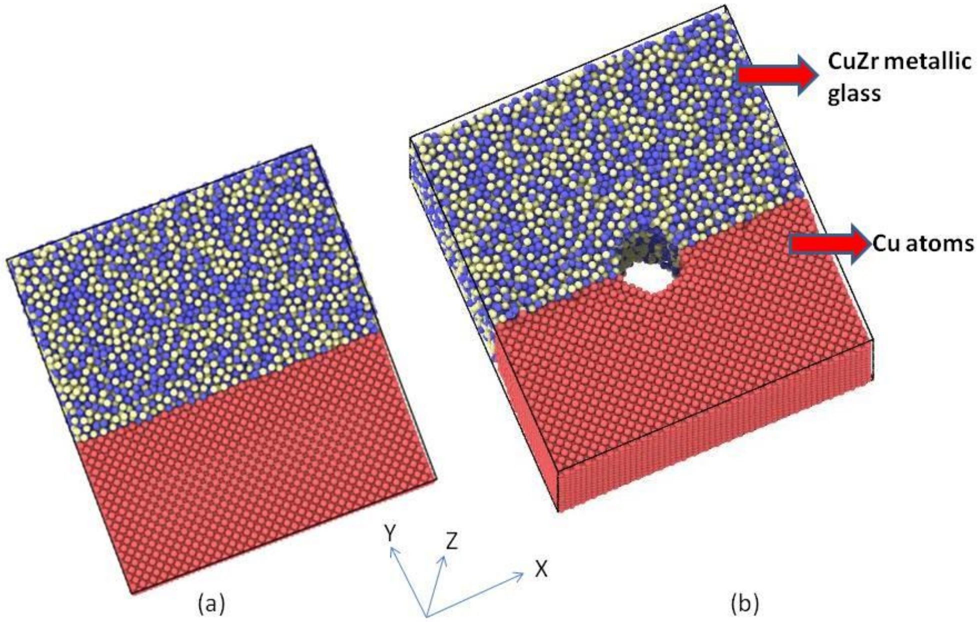

Figure 1. Atomic snapshot of interface (a) without crack, (b) with crack

4.3 EFFECT OF STRAIN RATE ON THE INTERFACE STRENGTH

To study the strain rate effect, three different strain rates are used in the simulation, which will predict the different properties of the interface. Stress-strain plot are plotted to examine the behaviour of the interface strength. Fig. 2 shows the (Mode-I without crack) stress-strain curves of interface at 100 K (Fig. 2a), at 300 K (Fig 2b) and 500 K (Fig 2c) and at three strain rates, i.e. 10^8 s^{-1}, 10^9 s^{-1} and 10^{10} s^{-1}. All the curves show a linear elastic and plastic behaviour. Yielding occurs by sudden drop in the stress. With further straining the stress-strain curves are serrated and are more prominent with decreasing strain rate and increasing temperature. With increasing strain rate, yield strength increases and decreases with increasing temperature.

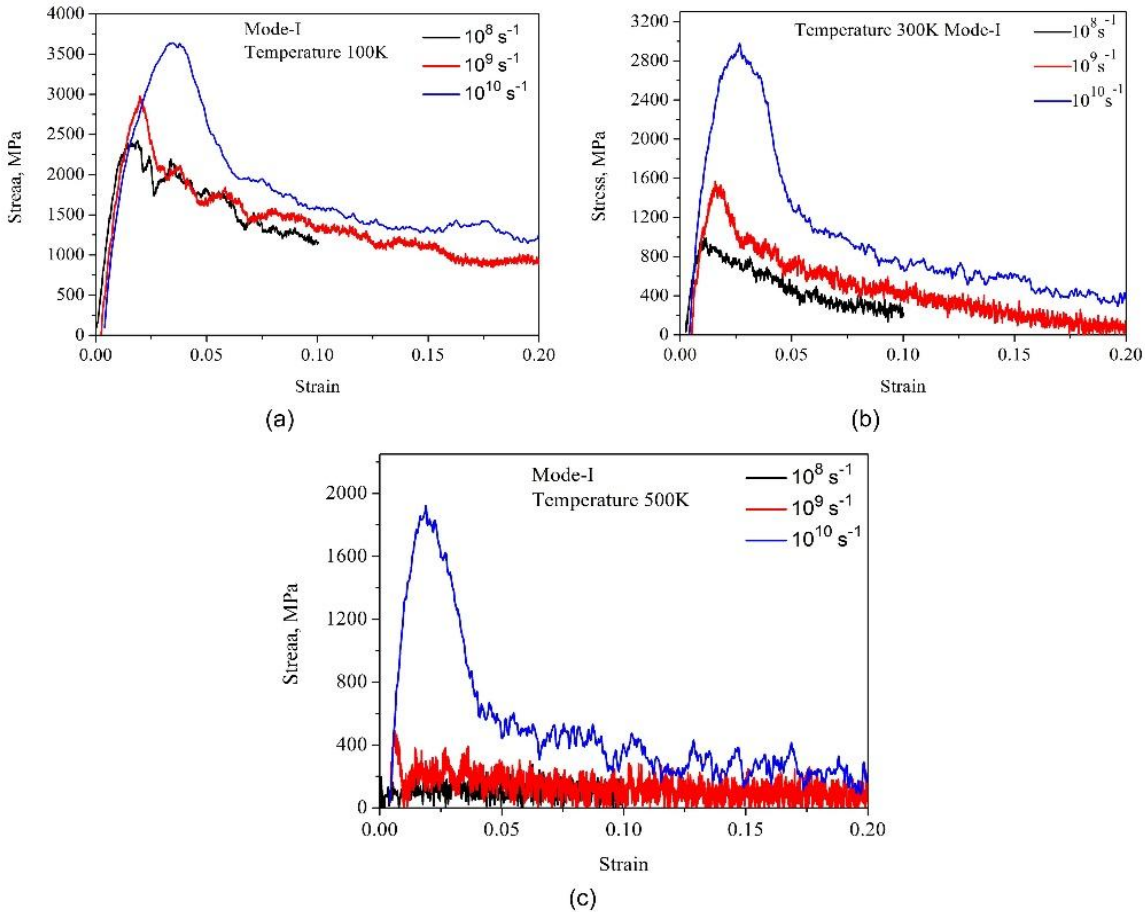

Figure. 2. Stress-Strain plot for Mode-I without crack, $Cu_{50}Zr_{50}$ metallic glass reinforced in Cu Metal matrix at varying strain rate from a to c; (a) 100K, (b**)** 300K, (c)500K.

4.3.1 Atomic positions snap shots (mode I deformation without crack)

The following Figs. 3a and 3b shows the atomic position snap shots of the model interface at different strains and deformed at stain rate of 10^{10} s^{-1} and 10^{9} s^{-1}. The plastic deformation initiates by slip in the crystalline region and by diffusive movement of atoms in the glassy region. With further straining (10%) a void is generated at the interface resulting in sudden drop in the stress.

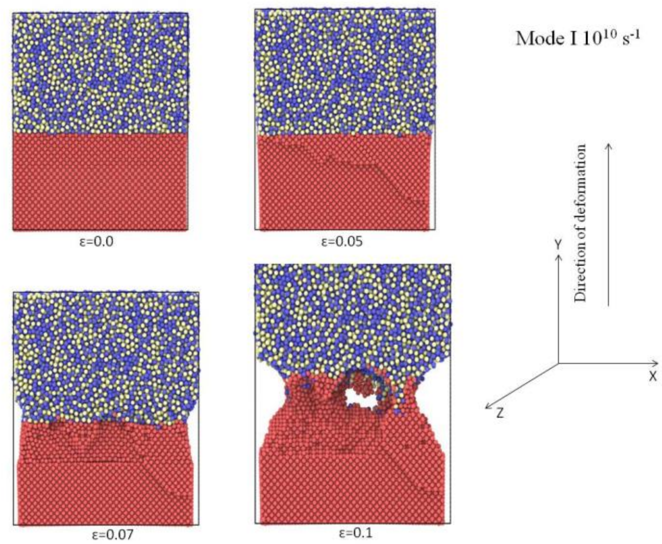

Figure. 3a: Atomic snapshot at different strains of the model without crack under Mode-I deformation strained at strain rate of $1 \times 10^{10} s^{-1}$.

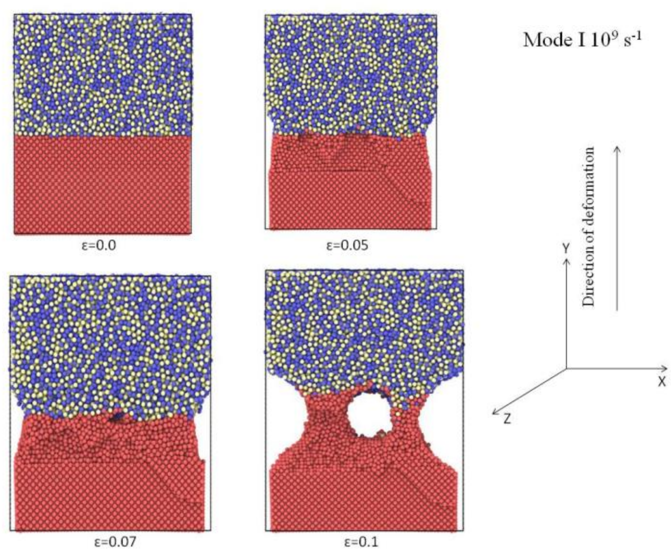

Figure. 3b: Atomic snapshot at different strains of the model without crack under Mode-I deformation strained at strain rate of $1 \times 10^{9} s^{-1}$.

Fig. 4 shows the (Mode-I with crack) stress-strain curves of interface at 100 K (Fig. 4a), at 300 K (Fig 4b) and 500 K (Fig 4c) and at three strain rates, i.e. $10^{8} s^{-1}$, $10^{9} s^{-1}$ and $10^{10} s^{-1}$. All the curves show a linear elastic and plastic behaviour. Yielding occurs by sudden drop in the stress. With further straining the stress-strain curves are serrated and are more prominent with decreasing strain rate and increasing temperature. With increasing strain rate, yield strength increases and decreases with increasing temperature.

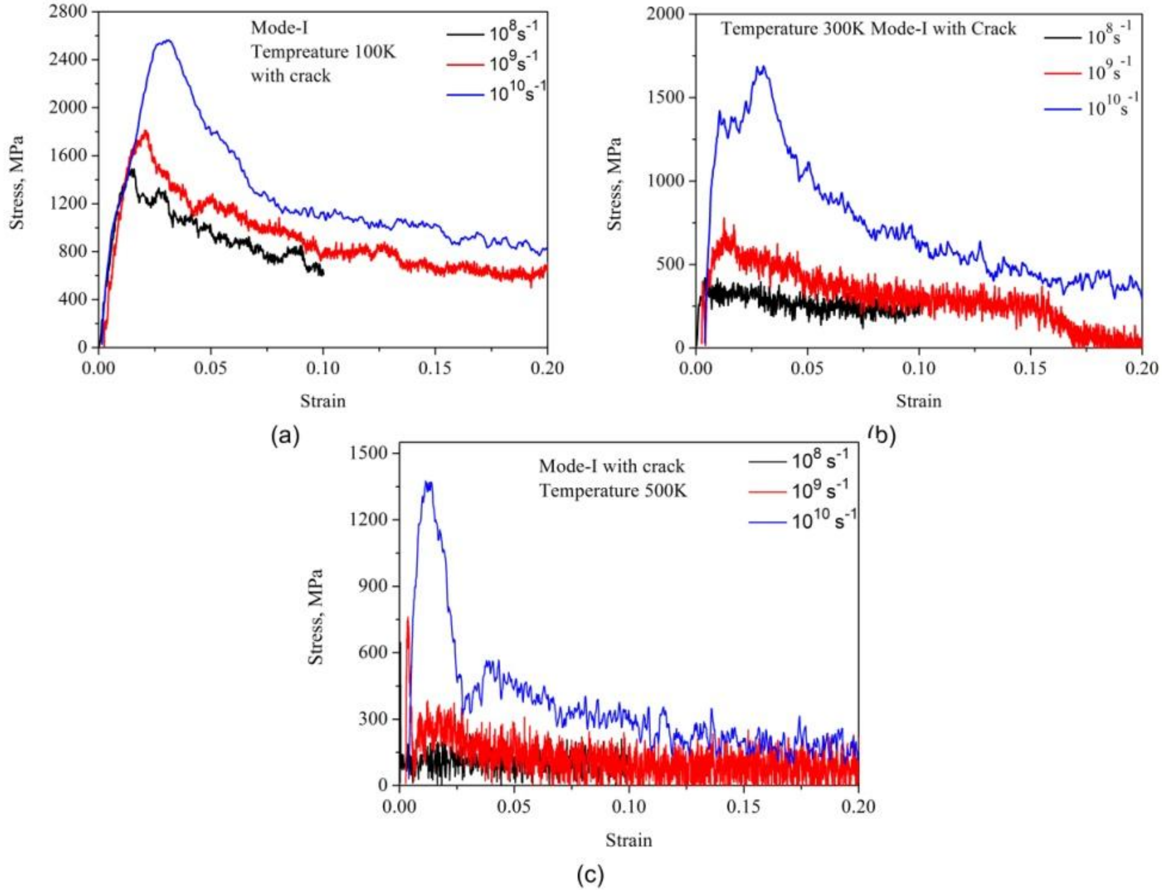

Figure. 4: Stress-Strain plot for Mode-I with crack, $Cu_{50}Zr_{50}$ metallic glass reinforced in Cu Metal matrix composite at varying strain rate from a to c; (a) 100K, (b) 300K, (c) 500K.

4.3.2 Atomic positions snap shots (mode I deformation of interface with crack)

The following Figs. 5a and 5b shows the atomic position snap shots of the model interface with crack at different strains and deformed at stain rate of 10^{10} s^{-1} and 10^9 s^{-1}. The plastic deformation initiates by slip in the crystalline region and by diffusive movement of atoms in the glassy region. The void enlarges with progress of deformation and separation of the interface occurs at strain of 0.16.

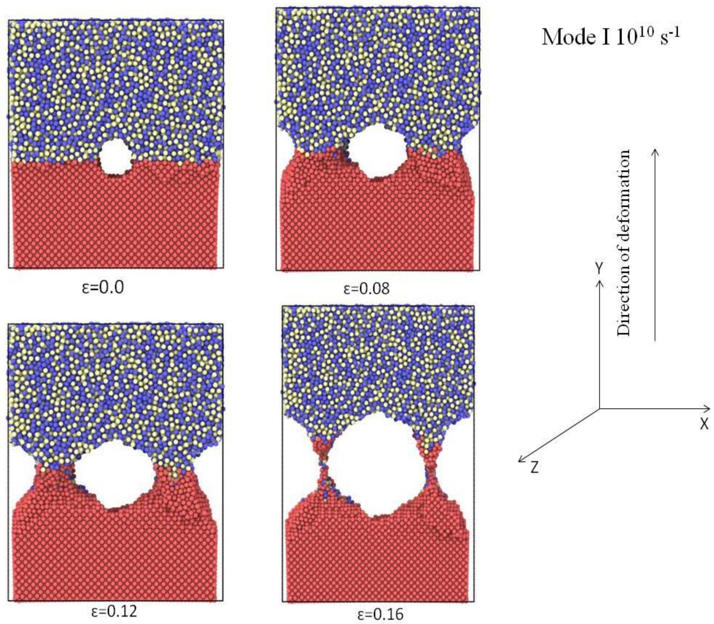

Figure 5a: Atomic snapshot at different strains of the model with crack under Mode-I deformation strained at strain rate of $1\times10^{10}\,s^{-1}$.

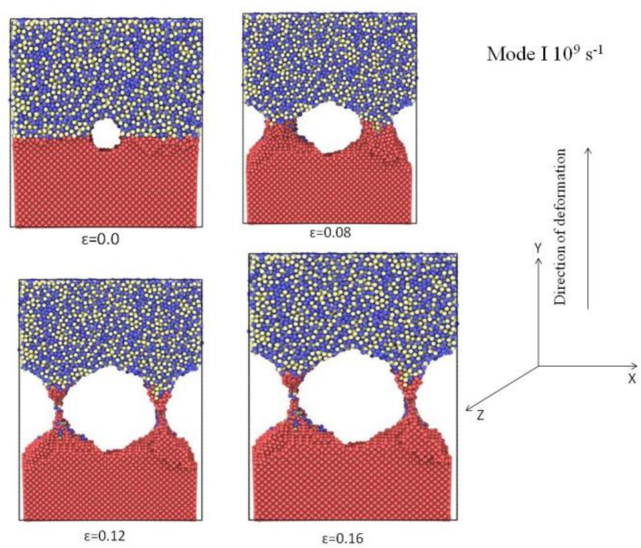

Figure 5b: Atomic snapshot at different strains of the model with crack under Mode-I deformation strained at strain rate of $1\times10^{9}\,s^{-1}$.

Fig. 6 shows the (Mode-II without crack) stress-strain curves of interface at 100 K (Fig. 6a), at 300 K (Fig 6b) and 500 K (Fig 6c) and at three strain rates, i.e. $10^8\,s^{-1}$, $10^9\,s^{-1}$ and $10^{10}\,s^{-1}$. All the curves show a linear elastic and plastic behaviour. Yielding occurs by sudden drop in the stress.

With further straining the stress-strain curves are serrated and are more prominent with decreasing strain rate and increasing temperature. With increasing strain rate, shear yield strength increases and decreases with increasing temperature.

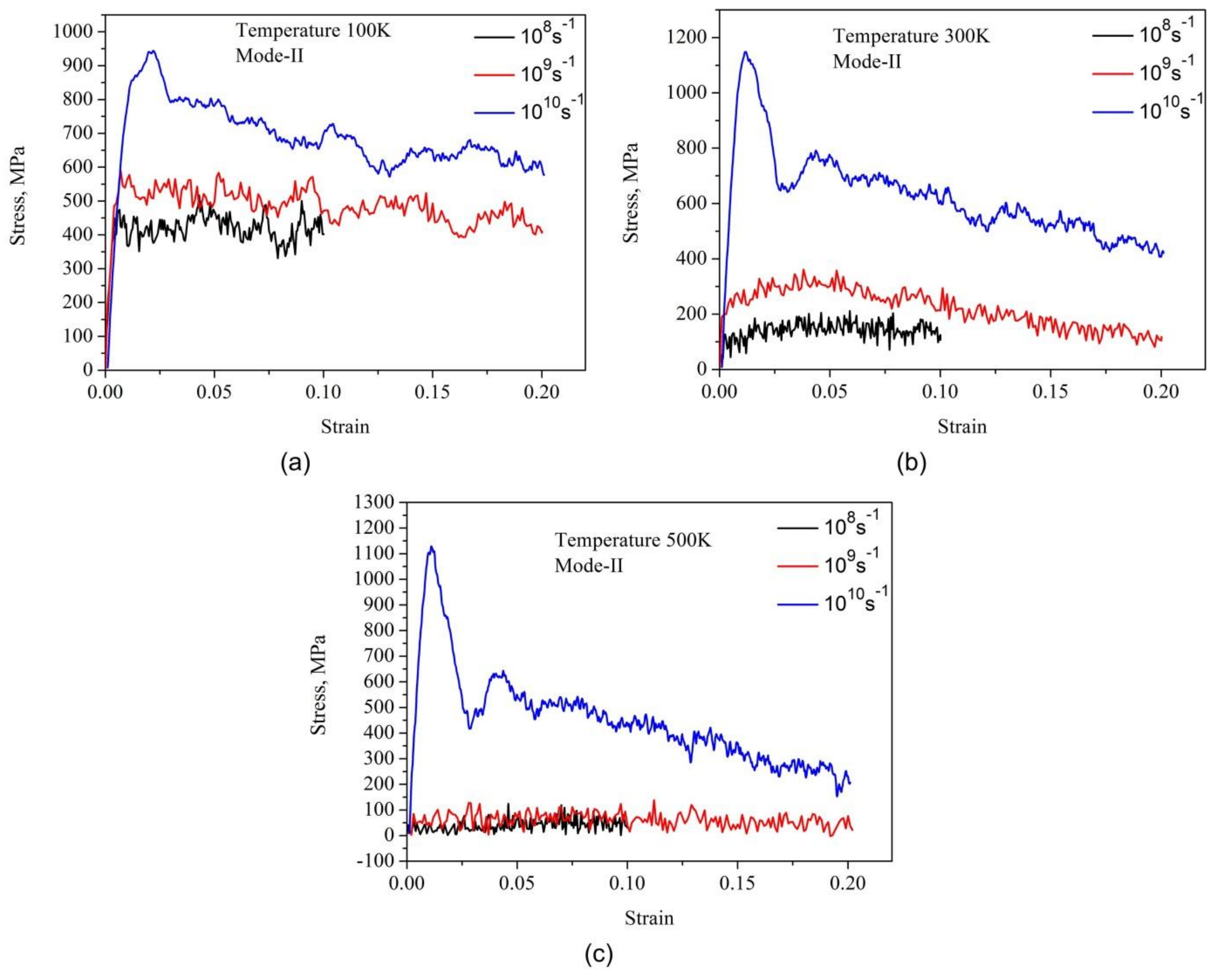

Figure. 6. Stress-Strain plot for Mode-II without crack, $Cu_{50}Zr_{50}$ metallic glass reinforced in Cu Metal matrix at varying strain rate from a to c; (a) 100K, (b) 300K, (c)500K.

4.3.3 Atomic positions snap shots (mode II deformation of interface without crack)

The following Figs. 7a and 7b shows the atomic position snap shots of the model interface at different strains and deformed at stain rate of 10^{10} s^{-1} and 10^{9} s^{-1}. The plastic deformation initiates by slip in the crystalline region and by diffusive movement of atoms in the glassy region. With progress of deformation amorphization of crystalline region occurs close to the interface at strain rate of 10^{9} s^{-1}.

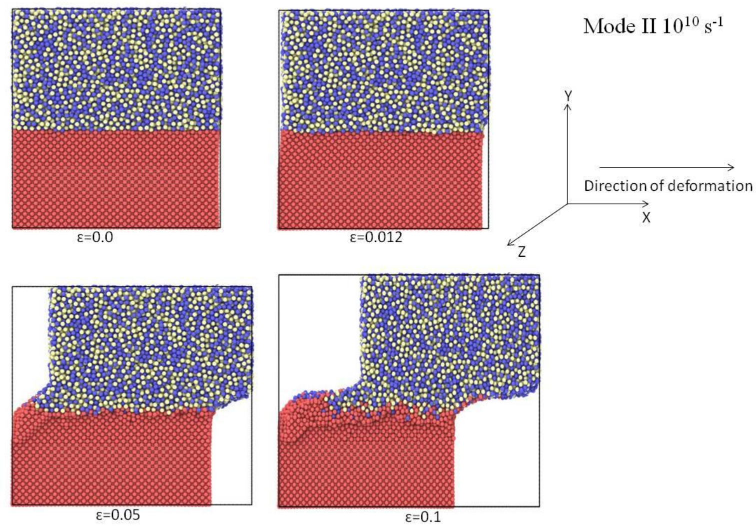

Figure 7a: Atomic snapshot at different strains of the model without crack under Mode-II deformation strained at strain rate of $1\times10^{10}\,s^{-1}$.

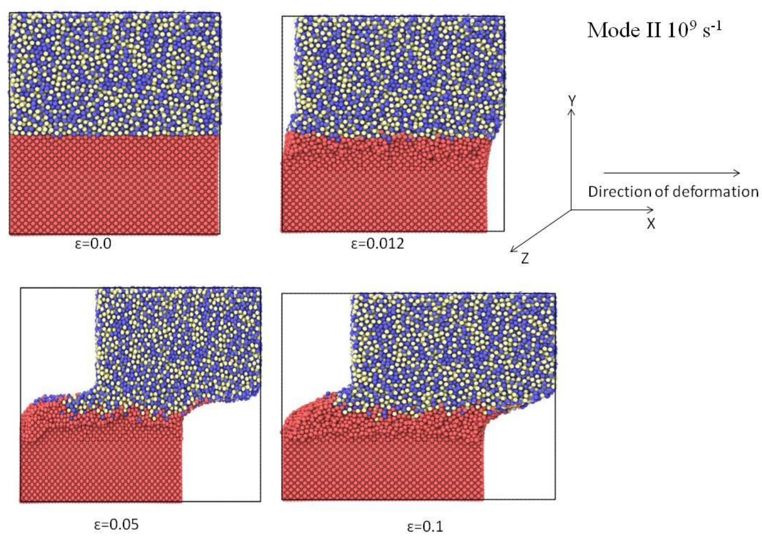

Figure 7b: Atomic snapshot at different strains of the model without crack under Mode-II deformation strained at strain rate of $1\times10^{9}\,s^{-1}$.

Fig. 8 shows the (Mode-II with crack) stress-strain curves of interface at 100 K (Fig. 8a), at 300 K (Fig 8b) and 500 K (Fig 8c) and at three strain rates, i.e. $10^8\,s^{-1}$, $10^9\,s^{-1}$ and $10^{10}\,s^{-1}$. All the curves show a linear elastic and plastic behaviour. Yielding occurs by sudden drop in the stress.

With further straining the stress-strain curves are serrated and are more prominent with decreasing strain rate and increasing temperature. With increasing strain rate, shear yield strength increases and decreases with increasing temperature.

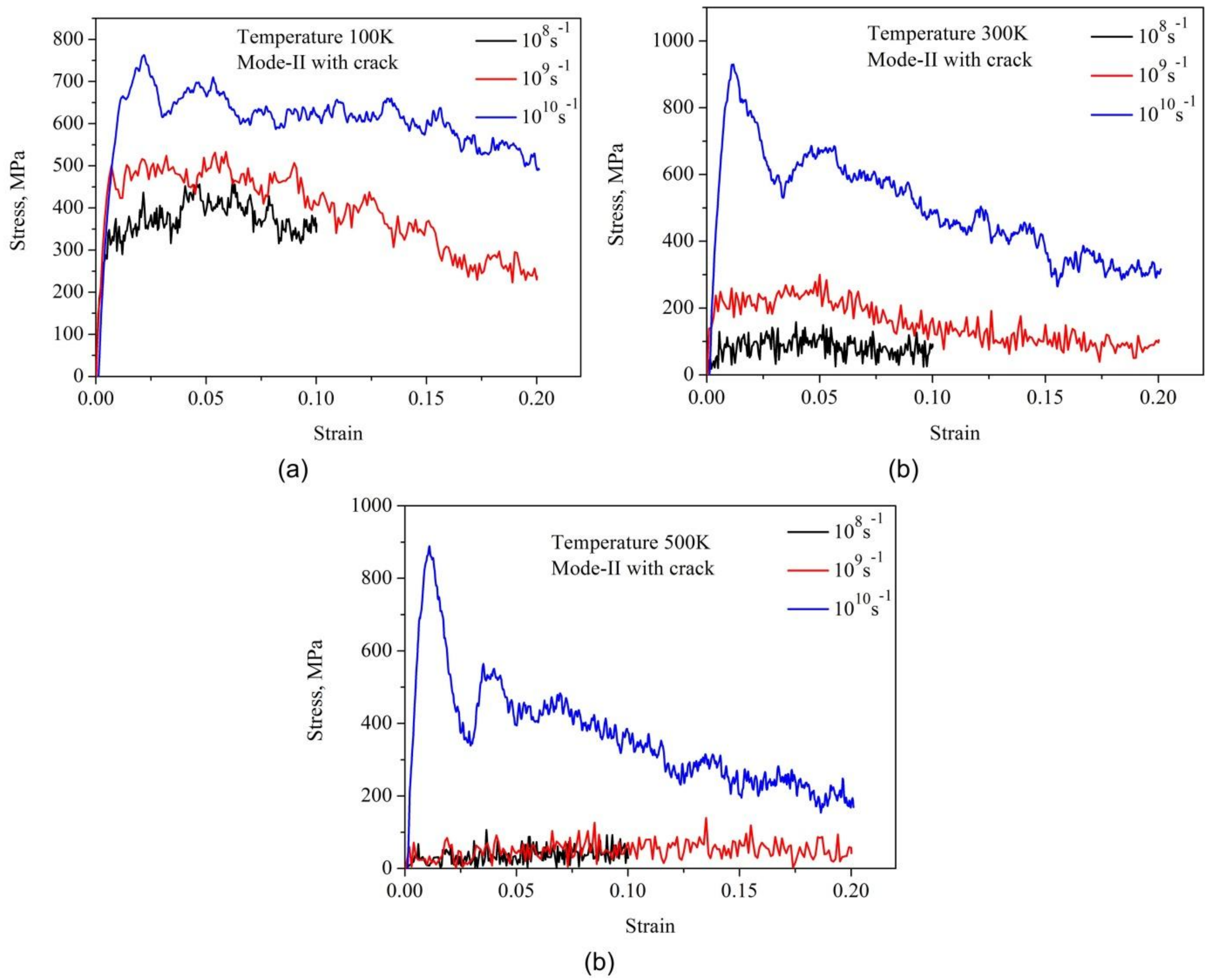

Figure. 8: Stress-Strain plot for Mode-II with crack, $Cu_{50}Zr_{50}$ metallic glass reinforced in Cu Metal matrix at varying strain rate from a to c; (a) 100K, (b**)** 300K, (c) 500K.

4.3.4 Atomic snap shots with crack (mode II deformation of interface with crack)

The following Figs. 8a and 8b shows the atomic position snap shots of the model interface at different strains and deformed at stain rate of 10^{10} s^{-1} and 10^{9} s^{-1}. The plastic deformation initiates by slip in the crystalline region and by diffusive movement of atoms in the glassy region. The regions near the void act as source of dislocations. With progress of deformation closure of the void occurs.

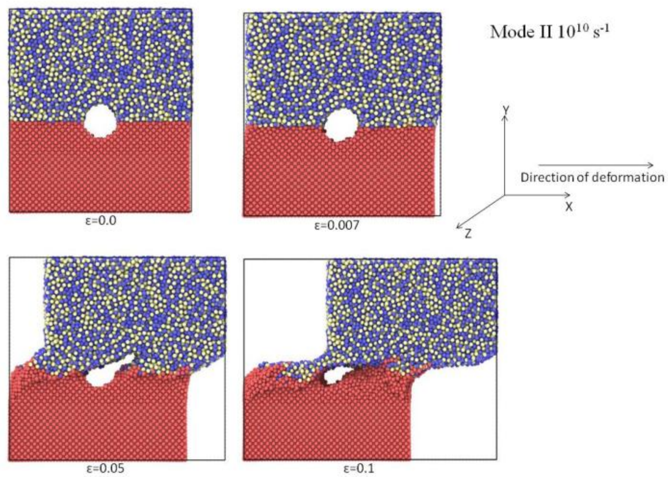

Figure 9a: Atomic snapshot at different strains of the model with crack under Mode-II deformation strained at strain rate of $1\times10^{10}\,s^{-1}$.

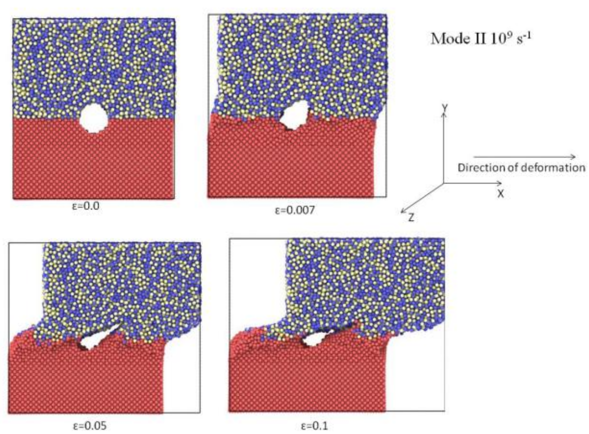

Figure 9b: Atomic snapshot at different strains of the model with crack under Mode-II deformation strained at strain rate of $1\times10^{9}\,s^{-1}$.

4.4 Effect of temperature on interface strength

Fig. 10 shows the (Mode-I without crack) stress-strain curves of the model interface at 10^8 s^{-1} (Fig.10a), at 10^9 s^{-1} (Fig 10b) and 10^{10} s^{-1} (Fig 10c) and at three different temperature, i.e., 100K, 300K and 500K. As the temperature increases the yield strength decreases. Flow softening is observed at all strain rates and temperatures.

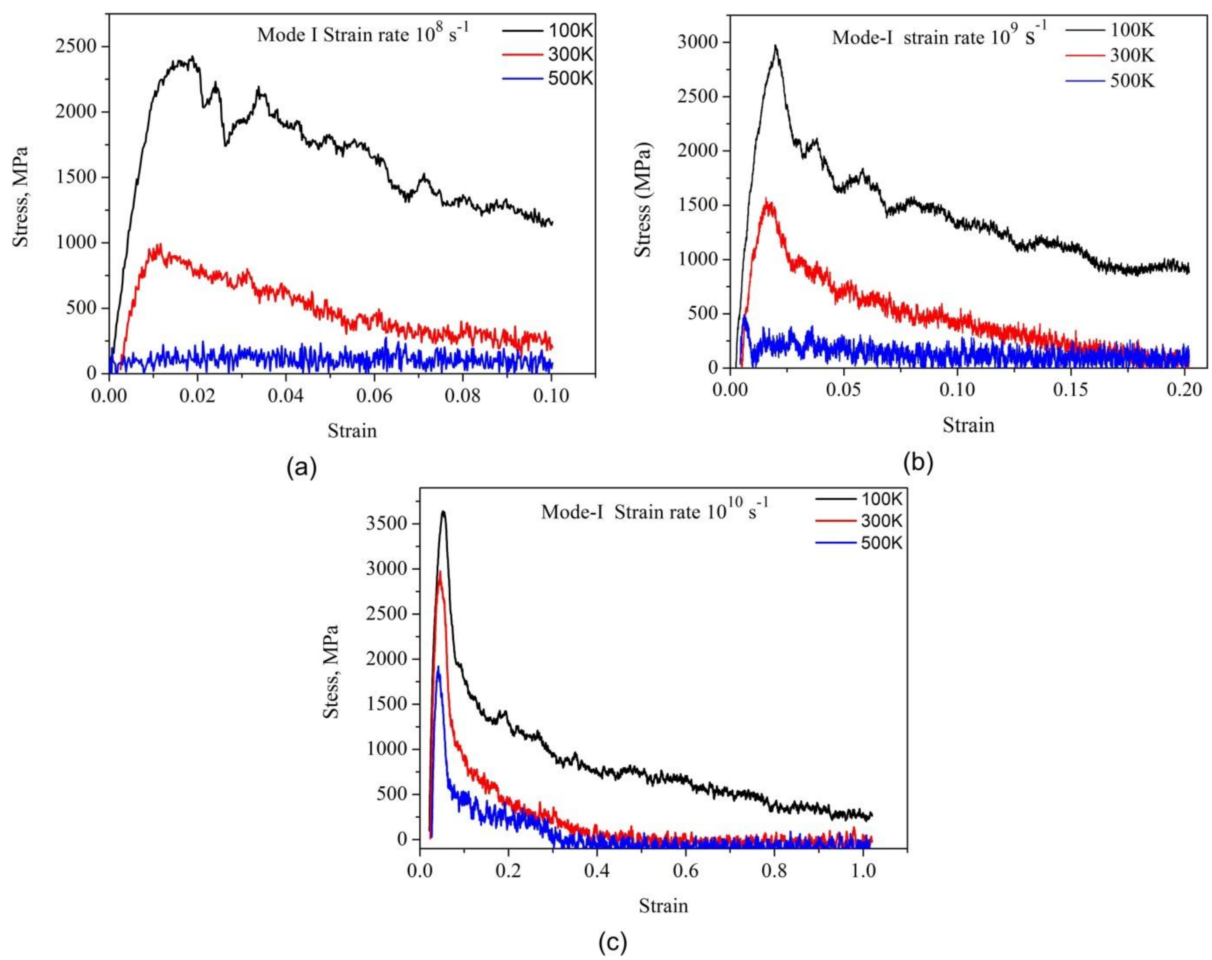

Figure 10: Stress-strain plot for Mode-I deformation of model interface without crack, at varying temperature from a to c (a) $1 \times 10^8 s^{-1}$, (b) $1 \times 10^9 s^{-1}$, (c) $1 \times 10^{10} s^{-1}$.

Fig. 11 shows the (Mode-I with crack) stress-strain curves of the model interface at 10^8 s^{-1} (Fig.11a), at 10^9 s^{-1} (Fig 11b) and 10^{10} s^{-1} (Fig 11c) and at three different temperature, i.e., 100K, 300K and 500K. As the temperature increases the yield strength decreases. Flow softening is observed at all strain rates and temperatures.

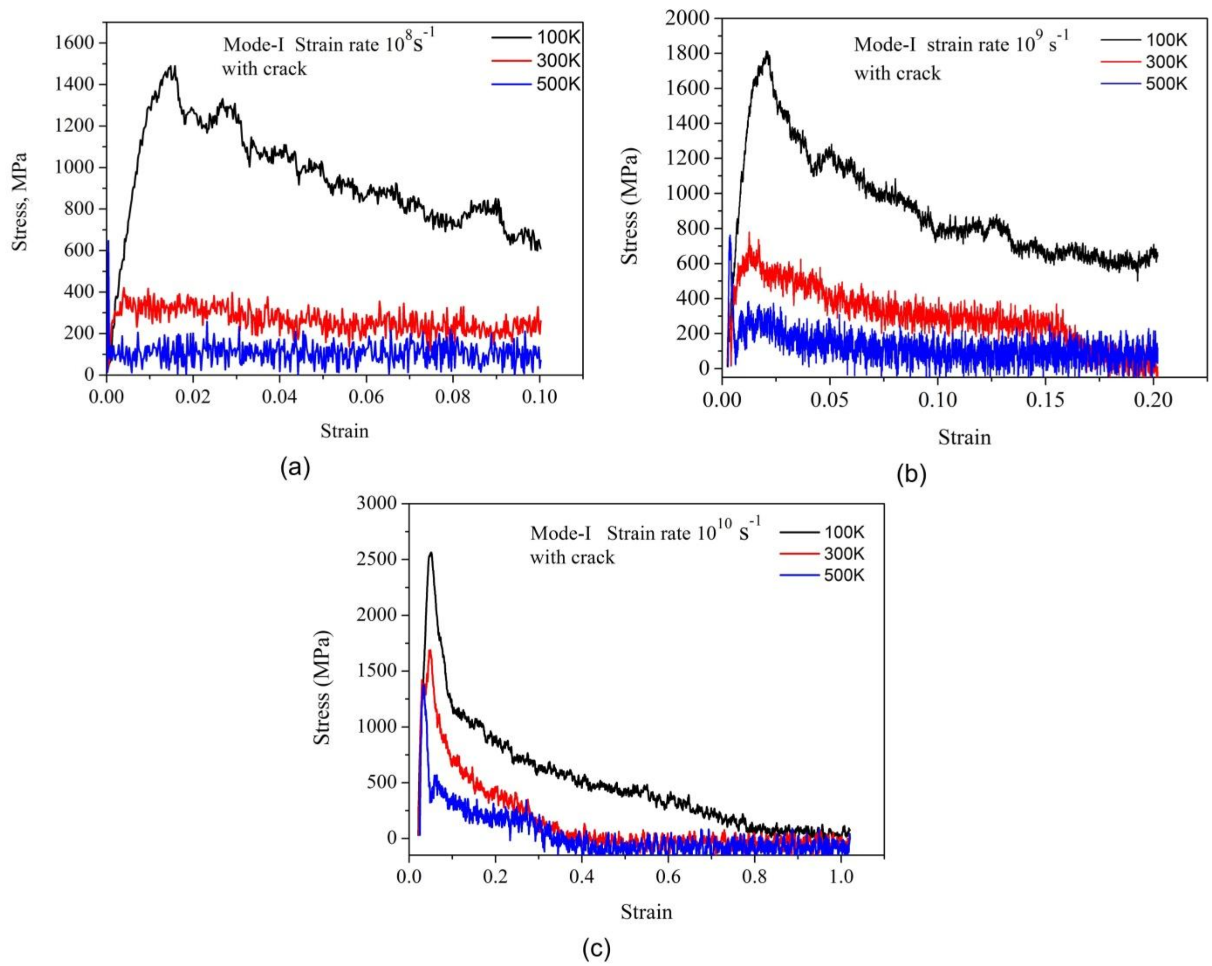

Figure 11: Stress-strain plot for Mode-I deformation of model interface with crack, at varying temperature from a to c (a) $1\times10^8 s^{-1}$, (b) $1\times10^9 s^{-1}$, (c) $1\times10^{10} s^{-1}$.

Fig. 12 shows the (Mode-II without crack) stress-strain curves of the model interface at 10^8 s^{-1} (Fig.12a), at 10^9 s^{-1} (Fig 12b) and 10^{10} s^{-1} (Fig 12c) and at three different temperature, i.e., 100K, 300K and 500K. As the temperature increases the yield strength decreases.

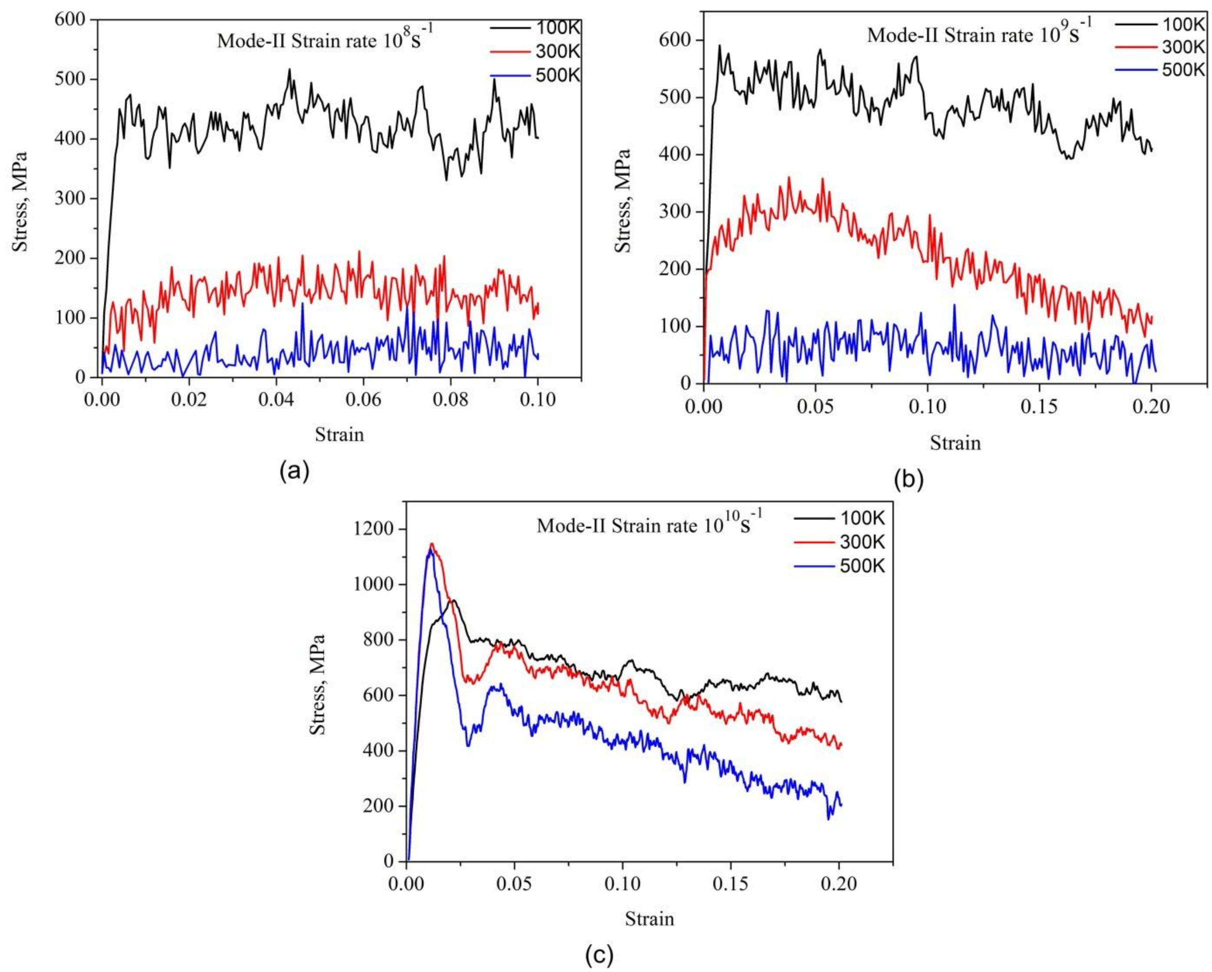

Figure 12: Stress-strain plot for Mode-II deformation of model interface without crack, at varying temperature from a to c (a) $1\times10^8 s^{-1}$, (b) $1 \times10^9 s^{-1}$, (c) $1\times10^{10} s^{-1}$.

Fig. 13 shows the (Mode-II with crack) stress-strain curves of the model interface at 10^8 s^{-1} (Fig.13a), at 10^9 s^{-1} (Fig 13b) and 10^{10} s^{-1} (Fig 13c) and at three different temperature, i.e., 100K, 300K and 500K. As the temperature increases the yield strength decreases.

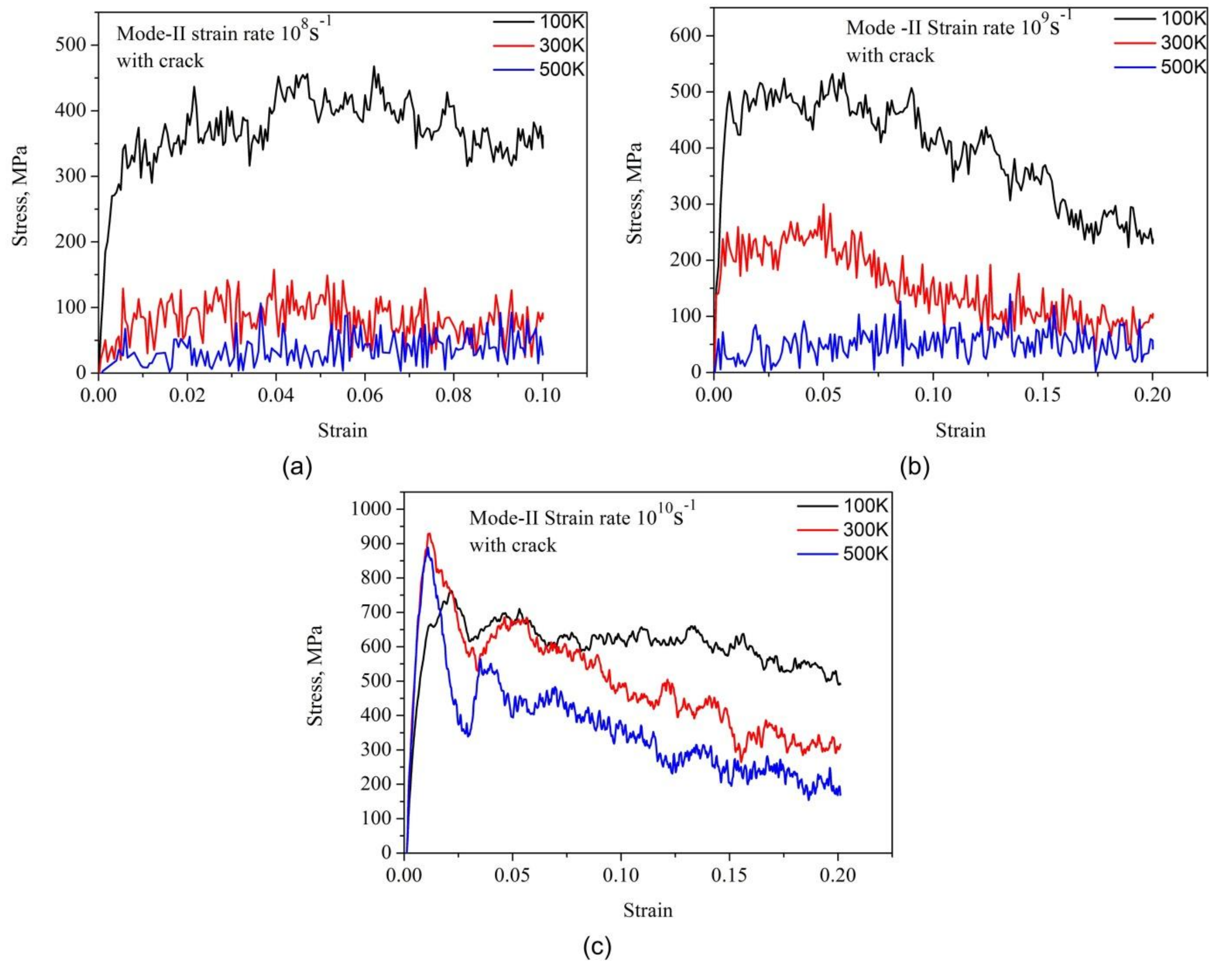

Figure 13: Stress-strain plot for Mode-II deformation of model interface with crack, at varying temperature from a to c (a) $1\times10^8 s^{-1}$, (b) $1\times10^9 s^{-1}$, (c) $1\times10^{10} s^{-1}$.

5. CONCLUSIONS

The present study gives a significant insight on the mechanism and deformation behaviour of the interface between $Cu_{50}Zr_{50}$ metallic glass reinforced in Cu Metal matrix composite. The stress-strain analysis provides vital information on the performance of these materials when they are used at different temperatures and loading conditions. The following conclusions can be drawn from the present study.

a) Plastic deformation mechanism is by slip (evident from atomic position snap shots) in the crystalline region and by random movement of atoms in the glassy region.
b) Yield strength increases with increase in strain rate, while decreases with increasing temperature.
c) Mechanical properties like Yield strength, ultimate tensile strength decreases with the presence of crack at the interface between $Cu_{50}Zr_{50}$ metallic glass reinforced in Cu Metal matrix composite.
d) Flow softening is observed at all strain rates and temperatures.

References

[1] Berner, A., et al. "Formation of nano-crystalline structure at the interface in Cu–C composite." Applied surface science 144 (1999): 677-681.

[2] Ashby, M. F., and A. L. Greer. "Metallic glasses as structural materials." Scripta Materialia 54.3 (2006): 321-326.

[3] Trexler, Morgana Martin, and Naresh N. Thadhani. "Mechanical properties of bulk metallic glasses." Progress in Materials Science 55.8 (2010): 759-839.

[4] Allen, Michael P. "Introduction to molecular dynamics simulation." Computational Soft Matter: From Synthetic Polymers to Proteins 23 (2004): 1-28.

[5] Berner, A., et al. "Microstructure of Cu–C interface in Cu-based metal matrix composite." Sensors and Actuators A: Physical 74.1 (1999): 86-90.

[6] Mondal, D. P., N. Ramakrishnan, and S. Das. "FEM modelling of the interface and its effect on the elastio-plastic behavior of metal matrix composites." Materials Science and Engineering: A 433.1 (2006): 286-290.

[7] Qing, Hai. "Micromechanical study of influence of interface strength on mechanical properties of metal matrix composites under uniaxial and biaxial tensile loadings." Computational Materials Science 89 (2014): 102-113.

[8] Deng, Kunjun, et al. "Atomistically derived metal–ceramic interfaces cohesive law based on the van der Waals force." Engineering Fracture Mechanics 111 (2013): 98 105.

[9] Dandekar, Chinmaya R., and Yung C. Shin. "Molecular dynamics based cohesive zone law for describing Al–SiC interface mechanics." Composites Part A: Applied Science and Manufacturing 42.4 (2011): 355-363.

[10] Rajan, T. P. D., R. M. Pillai, and B. C. Pai. "Reinforcement coatings and interfaces in aluminium metal matrix composites." Journal of Materials Science 33.14 (1998): 3491-3503.

[11] Yang, Zhenyu, et al. "Crack propagation behaviors at Cu/SiC interface by molecular dynamics simulation." Computational Materials Science 82 (2014): 17-25.

[12] Dandekar, Chinmaya R., and Yung C. Shin. "Effect of porosity on the interface behavior of an Al 2 O 3–aluminum composite: a molecular dynamics study." Composites Science and Technology 71.3 (2011): 350-356.

[13] Pavia, F., and W. A. Curtin. "Molecular modeling of cracks at interfaces in nanoceramic composites." Journal of the Mechanics and Physics of Solids 61.10 (2013): 1971-1982.

[14] Guo, Shi-Jun, et al. "Modeling of interface cracking in copper–graphite composites by MD and CFE method." Composites Part B: Engineering 58 (2014): 586-592.

[15] Berner, A., et al. "Formation of nano-crystalline structure at the interface in Cu–C composite." Applied surface science 144 (1999): 677-681.

[16] Yang, B. J., Y. Y. Hwang, and H. K. Lee. "Elastoplastic modeling of polymeric composites containing randomly located nanoparticles with an interface effect." Composite Structures 99 (2013): 123-130.

[17] Ward, D. K., W. A. Curtin, and Yue Qi. "Aluminum–silicon interfaces and nanocomposites: A molecular dynamics study." Composites science and technology 66.9 (2006): 1151-1161.

[18] Avishai, Amir, Christina Scheu, and Wayne D. Kaplan. "Intergranular films at metal–ceramic interfaces: Part I–interface structure and chemistry." Acta materialia 53.5 (2005): 1559-1569.

[19] Namilae, S., and Namas Chandra. "Role of atomic scale interfaces in the compressive behavior of carbon nanotubes in composites." Composites science and technology 66.13 (2006): 2030-2038.

[20] S. Plimpton, Fast Parallel Algorithms for Short-Range Molecular Dynamics, J Comp Phys, 117, 1-19 (1995)